Comparisons of Analytical and Experimental Measurements of Lamb Wave Interaction with Corrosion Damage in Aluminum Plates

E. D. SWENSON, C. T. OWENS, M. P DESIMIO and
S. E. OLSON

ABSTRACT

This paper presents an investigation of the interaction of guided elastic waves with chemically induced corrosion damage in an aluminum plate using a three-dimensional laser Doppler vibrometer (3D-LDV) and compares the measured wave fields to analytical predictions from finite element models (FEM). The investigation begins with 3D-LDV surface measurements of guided elastic waves propagating through an aluminum plate and interacting with corrosion damage in the plate. The elastic waves are created by applying a 5.5-cycle Hamming-windowed sine wave to a 6.35 mm piezoceramic disk bonded to the host structure using cyanoacrylate gage adhesive. The 3D-LDV measurements provide both in- and out-of-plane velocity components across a uniform grid of approximately 20,000 points with approximately 1 mm spacing between points in the x- and y-directions. Images created from the 3D-LDV measurements clearly show the interaction of the elastic wave energy with the corrosion damage and demonstrate that the presence, location, and amount of damage could be estimated. Comparisons of the out-of-plane velocity components from both the experimental measurements and analytical simulations provide positive indications that FEM techniques can model wave interaction with this particular form of corrosion damage in aluminum plates.

INTRODUCTION

This paper builds from an ealier investigation of the interaction of elastic waves with induced corrosion damage in an aluminum plate. The use of elastic waves has shown promise in detecting highly localized damage, such as cracking or delamination, due to the relatively short wavelengths of the propagating waves. Lamb waves offer several advantages for structural health monitoring (SHM), such

as the ability to propagate over relatively large distances, which improves the ability to monitor large areas for relatively small damage, and to provide through-thickness interrogation, which may be of particular importance when internal defects occur. Staszewski, *et al.* [2-5] and Owens, *et al.* [6-9] have demonstrated the potential of laser vibrometry to detect fatigue cracking in metallic structures.

The initial studies presented in this paper have been performed on an aluminum plate test article. Details on the experimental setup and laser vibrometer testing are provided. Experimental results are presented and compared against analytical predictions. Finally, conclusions and recommendations based on these studies are presented.

EXPERIMENTAL TESTING

The test article used for the initial studies is a sheet of 6061-T6 aluminum with a height of 609 mm, width of 609 mm, and thickness of 3.175 mm. One piezoelectric sensor is bonded to the center of one face of the plate using M-Bond 200 cyanoacrylate strain gage adhesive. The sensor is a 6.35 mm diameter piezoceramic disk with a thickness of 0.25 mm encapsulated in a Kapton protective layer that also contains electrical traces to provide or sense a voltage across the thickness of the sensor.

(a)   (b)
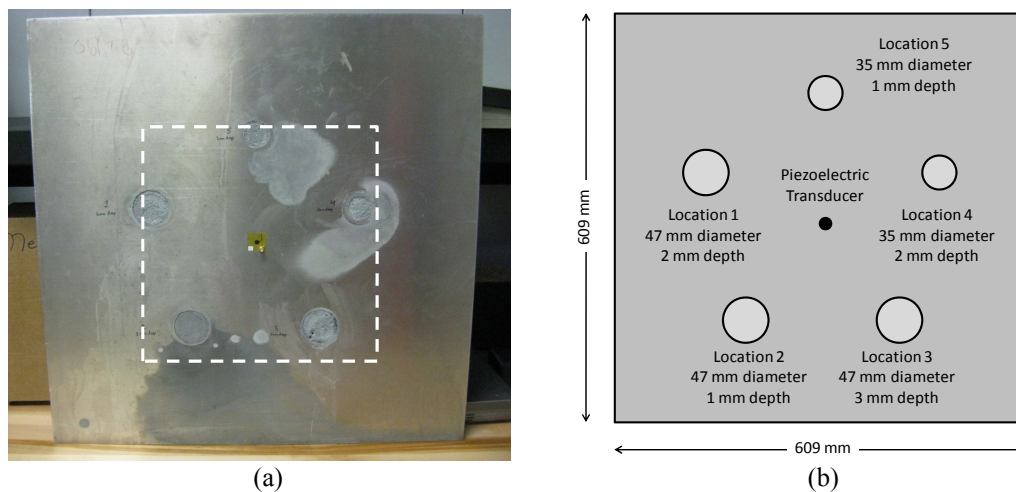
Figure 1. (a) Photograph of back side of test article and (b) schematic
identifying simulated corrosion areas (not to scale)

Figure 1 shows a photograph and schematic of the test article. Simulated corrosion has been created on one surface of the plate using a 30% hydrochloric acid solution. Varying the area of exposure, exposure time, and temperature provides depths of approximately 1.0, 2.0, and 3.0 mm at the locations shown in Figure 1(b), locations 2, 1, and 3, respectively. While five locations on the plate were subjected to hydrochloric acid in this experiment, only the three with a diameter of 47 mm will be discussed in this paper. Close-up photographs of the simulated corrosion areas are shown in Figure 2. Considerable variation in the surface texture can be seen, particularly for the areas with greater depths. For the 3.0 mm deep simulated corrosion area at Location 3, through holes are present at

several locations within the corroded region as seen in the lower left portions of Figure 2(c).

For the experimental testing, a Hamming-windowed, 5½-cycle sine burst excitation signal is generated using an Agilent 33120A waveform generator. A Krohn-Hite 7500 power amplifier is used to amplify the excitation signal to a peak-to-peak voltage of approximately 100 V and applied directly to the piezoelectric transducer. In prior experiments [10], pitch-catch testing was performed to create Lamb wave mode tuning curves to identify appropriate frequencies to generate A_0, S_0, or both modes. It was determined that excitation at a center frequency of 100 kHz dominantly excites the A_0 mode. A scanning laser Doppler vibrometer (LDV) is used to measure the elastic waves as they travel through the plate and interact with the damaged areas.
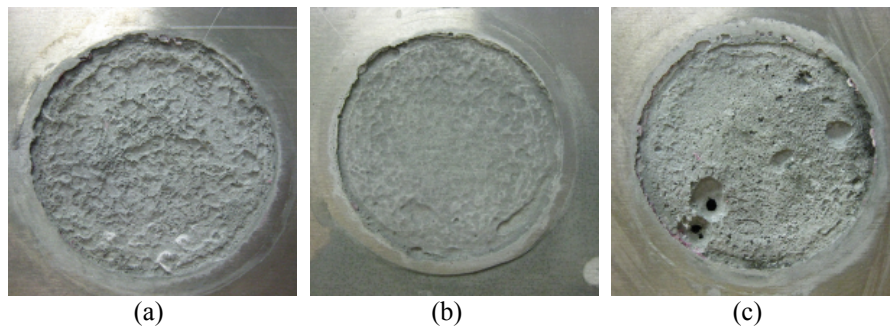

Figure 2. Close-up photographs of simulated corrosion damage at
(a) Location 1: 2 mm depth; (b) Location 2: 1 mm depth; and (c) Location 3: 3mm depth

Scanning LDV data collection is performed using a Polytec High Frequency PSV-400-3D-M Scanning Vibrometer system designed for full-field vibration measurements for frequencies up to 1 MHz. The system consists of a motorized PSV-A-T31 tripod, supporting three separate PSV-I-400 sensor heads, as well as a high-resolution camera that provides the capability to make precise corrections to the measurement points in 3D. Surface velocity measurements are made by evaluating the Doppler frequency shift of a laser beam reflected from the test article. For 3D measurements, surface velocities are recorded using three lasers coincident at a point on the surface of the plate. These measurements can be resolved onto a 3D orthogonal coordinate system after the measurement and laser head locations are determined through calibration procedures. Thus, the system allows for fast, precise, non-contact 3D measurements, with a complete resolution of 3D velocity vectors with respect to a Cartesian coordinate system. The face of the plate on the opposite side of the corrosion and sensor is scanned by the LDV. The region scanned by the laser is centered on each simulated corrosion damage region. In order to improve measurement accuracy (through increased laser energy return), retroreflective film is applied to the undamaged side of the plate.

During LDV scanning, measurements are taken over 100 mm by 160 mm scan region; however, only a 50 mm by 160 mm area is shown in the figures because the results are predominantly symmetric. For each measurement, 512 samples are collected at a 2.56 MHz sample rate, providing 200 μs of data. Uniform 1 mm grid spacing is utilized, resulting in scans containing approximately 20,000 measurement points. At each grid point, 40 responses are averaged to improve the signal to noise

ratio of the measurements. During averaging, an appropriate delay between each excitation allows responses to decay to levels similar to ambient noise. The results of the LDV measurements are velocity time histories at the set of specified grid locations on the scanned face of the plate.

FE models have been generated using ABAQUS/CAE, with simulations performed using ABAQUS/Explicit. The three locations in the plate are modeled using 3D linear solid elements. The transducer and adheseive layer are both modeled, and excitation is provided in the form of a time-varying voltage boundary condition. In order to minimize the total number of finite elements in the model, the symmetrical aspects of the problem were taken advantage of. The corrosion spots are modeled very simply as a reduction in plate thickness. Element sizes in the region of interest were chosen such that there are approximately 20 elements per wavelength. Element lengths are allowed to increase gradually from the region of interest to approximately 3 mm at the plate boundaries. The maximum allowable time step is chosen to match the experimental sample frequency of 2.56 MHz, providing more than 20 time steps per period.
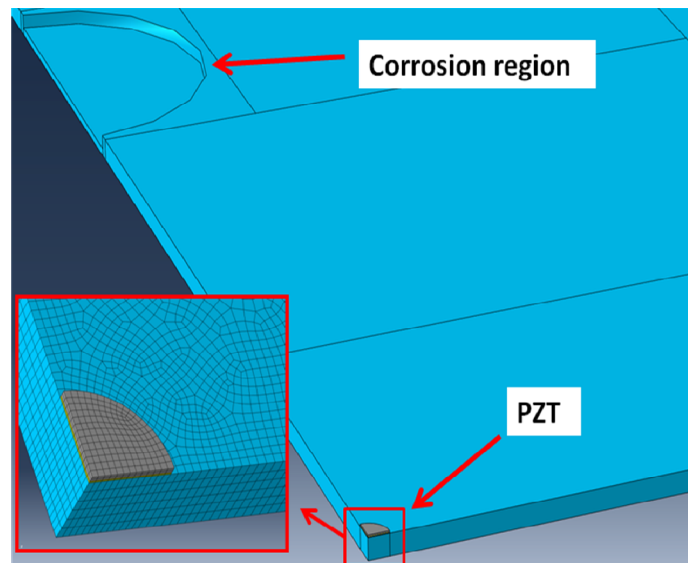

Figure 3. ABAQUS FE model showing PZT in the lower left and corrosion region in top left.

In order to maintain a good aspect ratio and have at least two elements through the thickness in the damaged region, models for the 1 and 2 mm deep corrosions sites have 6 elements through the thickness in the undamaged region of the plate and 4 and 2 elements through the thickness in the corroded regions, respectively. Both FE models have approximately 1.3 million degrees of freedom (DOF) and take 8 hours to run in parallel on 64 cores. For the 3 mm depth case, the model has 10 elements through the thickness in the undamaged region of the plate and 2 elements through thickness in the corroded region. This FE model has approximately 2.4 million DOF and run time is a little over 16 hours using 64 cores in parallel.

RESULTS

Out-of-plane velocity time histories of both the experimental and FE model results can be used to produce a time sequence of velocity field images showing elastic wave propagation across the plate including interaction with the damaged locations (see Fig. 4). The FE model images have been spatially re-sampled to match the measured experimental node locations, and all of the images are rotated to position the center of the corrosion region directly above the piezoelectric actuator, then only the right-half of the assumed symmetric zone is shown. Amplitude scaling and matching of the initial time histories of FE data are also performed for equitable comparison with the measured LDV results.
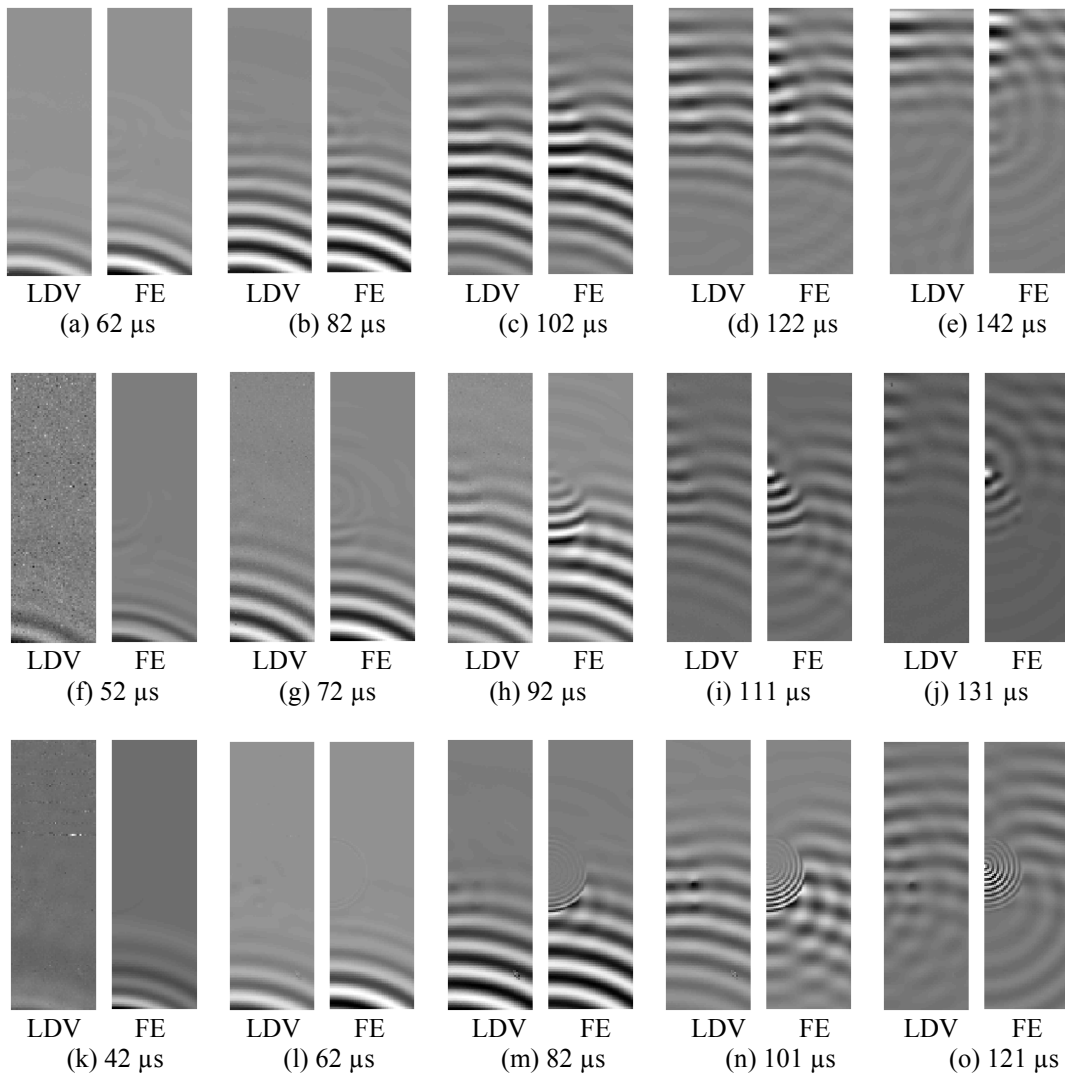

Figure 4. Processed out-of-plane velocity components from experimental LDV testing and FE model results for 100 kHz excitation at various times after the start of the excitation signal. Plots for the various corrosion depth cases, 1 mm: (a) – (e), 2 mm: (f) – (j), 3 mm: (k) – (o), are shown.

Propagation of the A_0 mode can clearly be observed in the sequence of images. Both the LDV and FE images show the A_0 waves entering each corroded region,

slowing as they propagate through the region, and then exiting the region. Location 3, with an approximate corrosion depth of 3 mm appears to have the largest slowing effect on the wave behavior due to the thickness change. The S_0 mode propagation is not evident in these out-of-plane images, but could contribute to the background noise seen in the images.

To better illustrate the effect of the simulated corrosion areas on the A_0 wave propagation, Figure 5 provides root mean square (RMS) plots of the right-half of the symmetric out-of plane velocity fields around each damage location for the majority of the time sequence. The existence of the circular corroded regions cause a focusing effect on the incident waves which is readily seen at the top left side of each subfigure. These regions indicate constructive interference which was seen in both the experimental and FE model results.

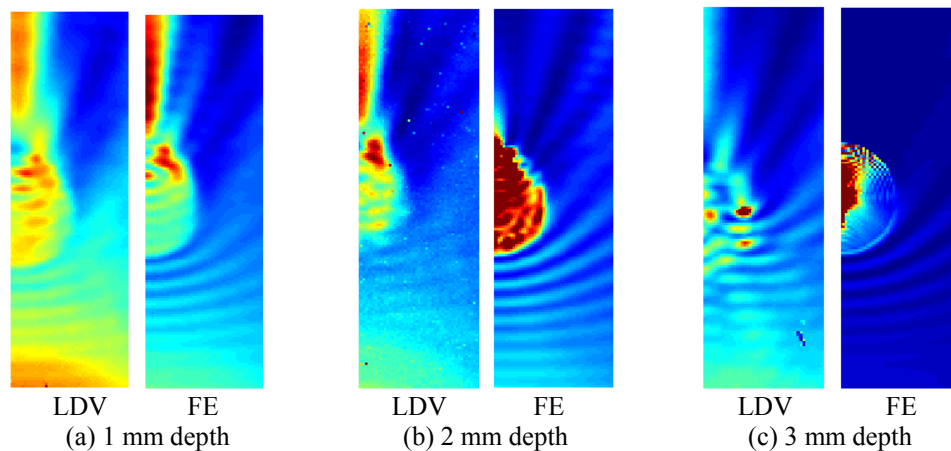| LDV   FE | LDV   FE | LDV   FE |
| (a) 1 mm depth | (b) 2 mm depth | (c) 3 mm depth |

Figure 5. Processed out-of-plane velocity root mean square (RMS) components around simulated corrosion locations for 100 kHz excitation for both analytical and experimental results

DISCUSSION

Processed images from the LDV scans and analytical results show that the simulated corrosion regions clearly affect elastic wave propagation. As shown in Figure 4, A_0 wave propagation at 100 kHz slows as the wave enters the corroded regions. At 100 kHz, the A_0 mode is operating in a range of the group velocity dispersion curve where changes to the frequency-thickness product can significantly affect the wave speed. Reflections from the front edge of the simulated circular corrosion damaged region can be seen in both Figures 4 and 5.

The measured and predicted FE results agree well for the 1 mm and 2 mm depth cases. Agreement between the measured and predicted FE results, particularly for wavelengths in the corroded region, is worse for the 3 mm thick case. This disagreement is possibly due to the low number of scanning points per wavelength (1 mm spacing between scan points when measuring an approximately 4 mm wavelength) and lack of FE modeling fidelity of the actual corroded regions. Figure 6 presents FE model results for out-of-plane velocity around the simulated 3 mm depth corrosion location at an arbitrary time. This image clearly illustrates the change in wavelength due to thickness change when the waves propagate across the simulated corrosion region.
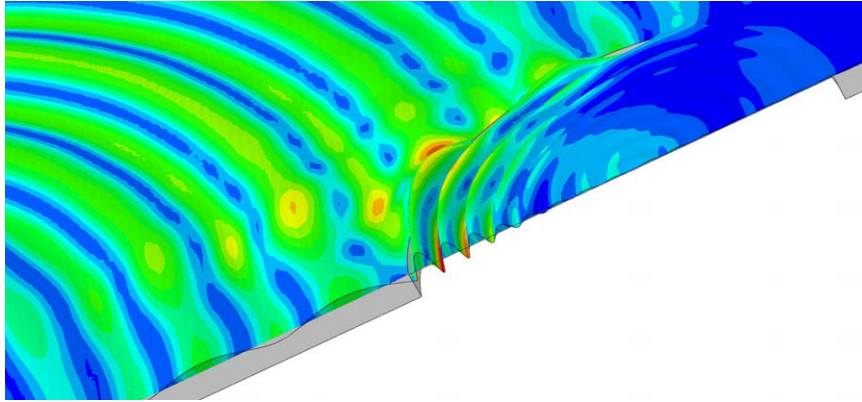
Figure 6. FE model results for out-of-plane velocity image around
simulated corrosion location for 100 kHz excitation

CONCLUSIONS

The use of elastic waves for corrosion detection has shown potential. This paper compares experimental and FE model results to investigate piezo-generated Lamb wave interaction with simulated corrosion damage. Scans of the out-of-plane velocity components of the A_0 mode at 100 kHz clearly indicate changes in the elastic wave fields caused by the simulated corrosion damage. Close agreement between the measured and predicted FE model results can be seen in the lightly damaged cases; however, agreement between the results is worse for the most severely damaged case. Further studies are warranted and should include consideration of both the A_0 and S_0 modes, as well as the in-plane velocity components.

ACKNOWLEDGMENTS

REFERENCES

1. Swenson, E.D., Olson, S.E., DeSimio, M.P., and Sohn, H., "Analysis of Lamb Wave Interaction with Corrosion Damage in Aluminum Plates," *Proceedings of the 5th Edition of the European Workshop on Structural Health Monitoring,* Naples-Italy, Jul. 2010.
2. Leong, W.H., W.J. Staszewski, B.C. Lee and F. Scarpa, "Structural health monitoring using scanning laser vibrometry: III. Lamb waves for fatigue crack detection," *Smart Materials and Structures*, 14, pp. 1387-1395, 2005.
3. Lee, B.C. and W.J. Staszewksi, "Lamb wave propagation modelling for damage detection: I. Two-dimensional analysis," *Smart Materials and Structures*, 16, pp. 249-259, 2007.
4. Lee, B.C. and W.J. Staszewski, "Lamb wave propagation modelling for damage detection: II. Damage monitoring strategy," *Smart Materials and Structures*, 16, pp. 260-274, 2007.

5. Staszewski, W.J., B.C. Lee and R. Traynor, "Fatigue crack detection in metallic structures with Lamb waves and 3D laser vibrometry," *Meas. Science and Technology*, 18, pp. 727-739, 2007.

6. Owens, C.T. and Swenson, E.D., "Comparison of Lamb Wave Interaction with High- and Low-Cycle Fatigue Cracks in Aluminum Plates" for *Proceedings of the 6th European Workshop on Structural Health Monitoring 2012,* Dresden, Germany, 3-6 July 2012.

7. Swenson, E.D., Owens, C.T., and Allen, C., "Interaction of Lamb Waves with Fatigue Cracks in Aluminum Plates" for *Proceedings of the 9th International Workshop on Structural Health Monitoring 2011,* Stanford, CA, 13-15 Sep 2011.

8. Owens, C.T., Swenson, E.D., and Allen, C. "Visualization of Lamb Wave Interaction with a 5 mm Fatigue Crack using 1D Ultra High Frequency Laser Doppler Vibrometry" for *Proceedings of the 9th International Workshop on Structural Health Monitoring 2011,* Stanford, CA, 13-15 Sep 2011.

9. Olson, S.E., DeSimio, M.P., Swenson, E.D., and Sohn, H., "Interaction of Lamb Waves with Structural Features of an Aircraft Fuselage," *Proceedings of the 5th Edition of the European Workshop on Structural Health Monitoring,* Naples-Italy, July. 2010.

10. Underwood, R., "Damage detection analysis using Lamb waves in restricted geometry for aerospace applications," Master's Thesis, Air Force Institute of Technology, March 2008.